J. Fluid Mech. (1966), *vol.* 25, *part* 3, *pp.* 437–456
Printed in Great Britain

Measurements of third-order resonant wave interactions

By L. F. McGOLDRICK,† O. M. PHILLIPS, N. E. HUANG AND T. H. HODGSON‡

The Department of Mechanics, The Johns Hopkins University, Baltimore, Maryland

(Received 19 July 1965)

This paper presents the results of experiments on the resonant interaction of gravity waves. Two mutually-orthogonal primary wave trains are generated in a tank and their interaction products studied at various positions on the surface. Under suitable conditions, the growing resonant third-order interaction product is identified; its amplitude is shown to be a linear function of the interaction distance. The band-width of the response decreases with increasing distance, as is characteristic of the phenomenon of resonance. The ratio of the frequencies of the primary waves at resonance is very close to that predicted theoretically; the growth rate of the third component is close to, though about 20 % higher than, the predicted value. Conditions far from resonance are also studied; it is found that the growing tertiary wave is absent in this case.

These results offer the first unambiguous experimental demonstration of resonant wave interactions.

1. Introduction

There has been a growing interest in recent years in the nature of the interaction process among the components of dispersive wave systems. One characteristic of such motions is that in each case, the wave-number $\mathbf{k}$ of any Fourier component is associated with a definite radian frequency $\sigma(\mathbf{k})$, a property not shared by, say, the components of a field of turbulence.§ If the wave amplitudes are small, the interactions are selective and weak: selective in that only certain combinations of wave components are capable of a significant energy interchange and weak because even for these, the interaction time is large compared with a typical wave period. If the wave-numbers $\mathbf{k}_1$, $\mathbf{k}_2$ and $\mathbf{k}_3$ are to participate in a continuous energy interchange, then it is necessary that the conditions

$$\left.\begin{aligned}\mathbf{k}_1 \pm \mathbf{k}_2 \pm \mathbf{k}_3 &= 0,\\ \sigma_1 \pm \sigma_2 \pm \sigma_3 &= 0,\end{aligned}\right\} \tag{1.1}$$

† Present address: The Department of the Geophysical Sciences, The University of Chicago, Chicago, Illinois.

‡ Present Address: Department of Aerodynamics, The College of Aeronautics, Cranfield, England.

§ If the waves are anisotropic, then $\sigma = \sigma(\mathbf{k})$. For example, in inertial waves, $\sigma = 2\mathbf{\Omega}\,.\mathbf{l}$, where $\mathbf{\Omega}$ is the angular velocity and $\mathbf{l}$ the unit vector $\mathbf{k}/k$.

be satisfied simultaneously, where $\sigma_i = \sigma_i(\mathbf{k}_i)$, $i = 1, 2, 3$ is the frequency associated with each wave-number. When these conditions are satisfied, the non-linear coupling between any two of the components generates a disturbance with the wave-number and frequency of a free wave mode (the third component) and energy is fed into this mode in a resonant manner.

The existence of this mechanism of resonant interaction was demonstrated theoretically by Phillips (1960) in a consideration of gravity waves in deep water. For these, however, in which $\sigma_i = (gk_i)^{\frac{1}{2}}$, it can be shown simply that there are no non-degenerate solutions to the binary interaction conditions (1.1), and it was necessary to examine the third-order interactions among four components. In this case, the resonance conditions are

$$\left.\begin{aligned} \mathbf{k}_1 \pm \mathbf{k}_2 \pm \mathbf{k}_3 \pm \mathbf{k}_4 &= 0, \\ \sigma_1 \pm \sigma_2 \pm \sigma_3 \pm \sigma_4 &= 0, \end{aligned}\right\} \tag{1.2}$$

and when $\sigma_i = (gk_i)^{\frac{1}{2}}$, it is found that there do exist non-trivial interactions among combinations of the type

$$\left.\begin{aligned} \mathbf{k}_1 - \mathbf{k}_2 &= \mathbf{k}_4 - \mathbf{k}_3, \\ \sigma_1 - \sigma_2 &= \sigma_4 - \sigma_3. \end{aligned}\right\} \tag{1.3}$$

Phillips, considering in particular the case $\mathbf{k}_1 = \mathbf{k}_3$, estimated the order of magnitude of the coupling coefficient and the initial rate of growth of the fourth component when its amplitude is initially zero. Subsequently, Longuet-Higgins (1962) devised an improved analysis which yielded a simple exact expression for the coupling coefficient, and Longuet-Higgins & Phillips (1962) showed that the same kind of interaction results in a second-order change in the phase velocity of any wave component in the presence of any other (any *pair* of wave-numbers $\mathbf{k}_1 \equiv \mathbf{k}_3$, $\mathbf{k}_2 \equiv \mathbf{k}_4$ evidently satisfying (1.3)). Later in that year, Benney (1962) obtained a closed set of equations to specify the development in time of all four slowly varying amplitudes $a_1(t), \ldots, a_4(t)$ of the wave components, and Bretherton (1964) found solutions to these in terms of elliptic functions.

Meanwhile, Hasselman (1962, 1963*a*, *b*) was involved with the statistical mechanics of the interactions among the components of a random, wind-generated ocean wave field and with the consequent modification in the shape of the wave spectrum. In other directions, Ball (1964) and S. Thorpe (1966) considered the resonant interactions between surface and internal gravity waves modes, McGoldrick (1965) the second-order energy interchanges among gravity-capillary waves and B. A. Hughes (also yet unpublished) the same phenomenon in the context of inertial waves in a uniformly rotating fluid. It might also be mentioned that Pierson (1961) has expressed the opinion that the whole concept of resonant wave interactions is fallacious and, as a result, something of a controversy has ensued. In any event, against the development of this growing body of theory there has been, to our knowledge, no direct experimental evidence for the existence of this type of resonant interaction nor any clear observational assessment of the predictions of the theory. It was to remedy this deficit that the present measurements were undertaken.

The experiment is very similar to the one suggested by Longuet-Higgins (1962). Two wave trains (the primary waves) are generated by plungers on adjacent sides of a square wave tank; at one particular frequency ratio the resonance conditions are satisfied and a tertiary wave, whose initial amplitude is zero, grows with distance across the tank. The detection and measurement of this third wave posed a number of problems and more than two years elapsed before they were resolved to our satisfaction. As a result of the rather small size of our wave tank, the time available for the interaction was limited to about ten wave periods, much less than the characteristic interaction time. The tertiary wave, whose initial amplitude was zero, is then everywhere small compared with the primary waves; to resolve it required very sharp filters and, on account of the relatively low frequencies involved, very long averaging times. The wave probes and the associated equipment were required to have a response very closely linear, to avoid the appearance of spurious harmonics. Finally, of course, the measurements had to be repeatable. Longuet-Higgins & Smith did in fact attempt an experiment of this kind, but their results were, until now, not published.† Nevertheless, it is a pleasure to acknowledge our indebtedness to them for an early description of their own work in this direction.

Before we enter into a detailed description of the experiment, some aspects of the theory of this particular interaction should be outlined a little more explicitly.

2. The theory of the interaction

Consider, first, a set of four interacting gravity wave trains in which the velocity potential is represented by

$$\phi = \left\{ \sum_{r=1}^{4} b_r(t)\, e^{k_r z}\, e^{i\chi} \right\} + \hat{\phi}, \tag{2.1}$$

where $\chi = \mathbf{k}_r . \mathbf{x} - \sigma_r t$ are such that the resonance conditions (1.3) are satisfied, and $\hat{\phi}$ represents the bounded second- and third-order contributions to the velocity potential resulting from the interaction. The complex first-order magnitudes b_r are slowly varying functions of time in the sense that

$$\left| \frac{db_r}{dt} \right| \ll \sigma_r |b_r|. \tag{2.2}$$

To the first order, the kinematic free-surface condition is $\dot{\zeta} = \partial\phi/\partial z$, where $\zeta(x,y,t)$ is the free-surface displacement. In virtue of this, the amplitude of each wave component is

$$a_r = ik_r b_r/\sigma_r \quad (r = 1, \ldots, 4), \tag{2.3}$$

to the first order. The first-order terms of (2.1) satisfy Laplace's equation as they stand; when the dynamical and kinematical free-surface conditions are

† Because of the close connexion between this study and ours, they are here being published together.

expanded to the third order and the substitution (2.1) is made, there results the following set of equations specifying the ratio of change of the quantities b_r:

$$\left.\begin{aligned} \sigma_1 \dot{b}_1 &= ib_1 \sum_{s=1}^{4} g_{1s} b_s b_s^* + ihb_2 b_3 b_4^*, \\ \sigma_2 \dot{b}_2 &= ib_2 \sum_{s=1}^{4} g_{2s} b_s b_s^* + ihb_1 b_3^* b_4, \\ \sigma_3 \dot{b}_3 &= ib_3 \sum_{s=1}^{4} g_{3s} b_s b_s^* + ihb_1 b_2^* b_4, \\ \sigma_4 \dot{b}_4 &= ib_4 \sum_{s=1}^{4} g_{4s} b_s b_s^* + ihb_1^* b_2 b_3. \end{aligned}\right\} \tag{2.4}$$

The derivation is given, in essence, by Benney (1962) though he slightly misstated the resonance condition and, as a result, his equations are slightly different in detail. The real coefficients g_{rs} $(r, s = 1, \ldots, 4)$ and h are constants of the interaction and are functions of the configuration of vectors $\mathbf{k}_1 \ldots \mathbf{k}_4$.

The terms involving g_{rs} are associated with changes in the phase velocity that result from self and mutual interactions. The diagonal terms whose coefficients are simply

$$g_{rr} = \tfrac{1}{2}k_r^4 \quad (r = 1, \ldots, 4) \text{ (no summation)}$$

describe the interaction of a wave with itself to the third order, which produces the increase in phase velocity of $\frac{1}{2}(k_r a_r)^2 (g/k_r)^{\frac{1}{2}}$ (no summation) found by Stokes. The off-diagonal terms in the matrix $\underset{\sim}{g}$ specify changes in the phase velocity resulting from the mutual interaction between pairs of waves, an effect noted by Longuet-Higgins & Phillips (1962). These authors give expressions for the coefficients g_{rs}, which are rather complicated functions of the vectors $\mathbf{k}_r$ and $\mathbf{k}_s$ of the order $k_r^2 k_s^2$. It is the remaining term in each equation that describes the energy interchange among the components, the identification and measurement of which is the object of the experiment.

Of all the possible resonant configurations of the vectors $\mathbf{k}_1 \ldots, \mathbf{k}_4$, one is particularly convenient for experimental study. This is illustrated in figure 1. Two of the primary wave trains coincide (say $\mathbf{k}_3 = \mathbf{k}_1$) and are perpendicular to another ($\mathbf{k}_2$) so that there are only three distinct wave-numbers in the interacting quarter. The interaction equations for this case are found by taking the limit $\mathbf{k}_3 \to \mathbf{k}_1$, the relative phase of b_3 and b_1 in the interaction region being such that the local momentum and energy densities are continuous as the limit is approached. This requires that $b_3 = ib_1$ and the velocity potential in the now combined single wave is specified through (2.1) by $\hat{b}_1 = (1+i)\, b_1$. When $k_1 = k_3$, the coefficients $g_{1s} = g_{3s}$ and $g_{r1} = g_{r3}$ and the interaction equation (2.4) become

$$\left.\begin{aligned} \sigma_1 \dot{\hat{b}}_1 &= i\hat{b}_1 (g_{11} \hat{b}_1 \hat{b}_1^* + g_{12} b_2 b_2^* + g_{14} b_4 b_4^*) + ih\hat{b}_1^* b_2 b_4, \\ \sigma_2 \dot{b}_2 &= ib_2 (g_{21} \hat{b}_1 \hat{b}_1^* + g_{22} b_2 b_2^* + g_{23} b_4 b_4^*) + \tfrac{1}{2} ih\hat{b}_1^2 b_4^*, \\ \sigma_4 \dot{b}_4 &= ib_4 (g_{41} \hat{b}_1 \hat{b}_1^* + g_{42} b_2 b_2^* + g_{44} b_4 b_4^*) + \tfrac{1}{2} ih\hat{b}_1^2 b_2^*, \end{aligned}\right\} \tag{2.5}$$

the first and last of the set (2.4) being now identical. The coupling coefficient h in this case of two coincident wave-numbers is given by Longuet-Higgins' (1962) analysis as

$$h = k_1^3 k_2 (1 + \xi)\, F(\xi), \tag{2.6}$$

where
$$\xi = (\sigma_2-\sigma_1)/\sigma_1 \tag{2.7}$$
and
$$F(\xi) = \frac{(1+\frac{1}{2}\xi^2)^2(1-4\xi^2)}{(1+\xi)^2}\left[1+\frac{4\xi}{\xi-(6+\xi^2)^{\frac{1}{2}}}\right]. \tag{2.8}$$

When, as in these experiments, $\mathbf{k}_1$ and $\mathbf{k}_2$ are mutually perpendicular, resonance is found at the frequency ratio $\sigma_1/\sigma_2 = 1{\cdot}7356$, whence $\xi = -0{\cdot}424$ and $F(\xi) \simeq 0{\cdot}312$.

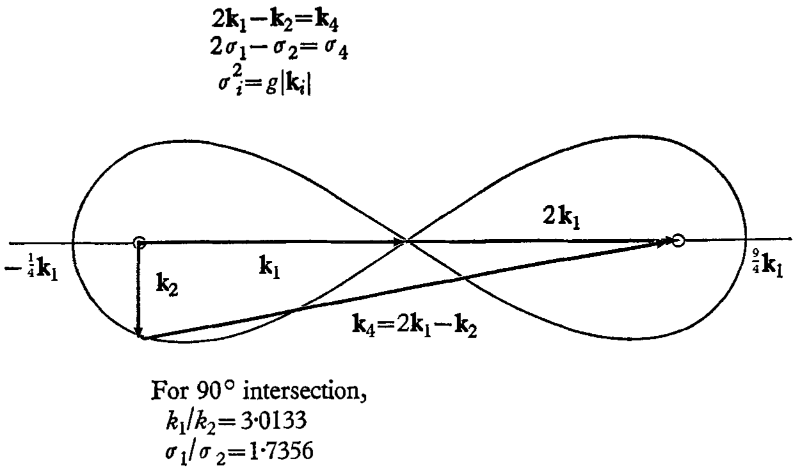

FIGURE 1. Solutions to the resonance conditions.

In the tank, the third component, whose amplitude is initially zero, builds up solely as a result of the energy transfer. Two energy partition integrals can be found simply from (2.5):

$$\left.\begin{aligned}\sigma_1 b_1 b_1^* + 2\sigma_2 b_2 b_2^* &= \text{const.},\\ \sigma_1 b_1 b_1^* + 2\sigma_4 b_4 b_4^* &= \text{const.}\end{aligned}\right\} \tag{2.9}$$

Consequently, the initial growth of the component with wave-number $\mathbf{k}_4$ is accompanied by an increase in the energy density of the $\mathbf{k}_2$-component, *both* at the expense of the $\mathbf{k}_1$-component. Throughout the tank, however, $|b_4|$ is small compared with either $|b_1|$ or $|b_2|$ which are both sensibly constant, and for the present purpose, it is sufficient to approximate the third member of (2.5) by

$$\sigma_4\dot{b}_4 = \tfrac{1}{2}ihb_1^2b_2^*, \tag{2.10}$$

where the circumflex is dropped from $\hat{b}_1$. Consequently,

$$b_4 = \frac{ihb_1^2b_2^*}{2\sigma_4}t.$$

The wave amplitudes $a_r = ik_r b_r/\sigma_r$ (no summation), so that

$$\begin{aligned}|a_4| &= \frac{h}{2g}\frac{\sigma_1^2\sigma_2}{k_1^2k_2}|a_1^2|\,|a_2|\,t\\ &= \tfrac{1}{2}k_1^2\sigma_2(1+\xi)\,F(\xi)\,|a_1^2|\,|a_2|\,t,\end{aligned} \tag{2.11}$$

since $\sigma_1^2 = gk_1$ and from (2.6). In our experiments the interaction time t is represented by the distance $d = tc_g$ over which the interaction has taken place, where c_g is the group velocity of the growing tertiary wave. Equation (2.11) can be written alternatively as

$$a_4/d = (a_1k_1)^2(a_2k_2)\,G(r,\theta), \tag{2.12}$$

where $G = (\sigma_3/\sigma_2)(1+\xi)F(\xi)$, $r = \sigma_1/\sigma_2 = (\xi+1)^{-1}$ and θ is the angle of intersection of the primary waves. At resonance, of course, r (and so ξ) is a function of θ.

Two further points should be noted. First, the ratio $\sigma_1/\sigma_2 = 1{\cdot}7356\ldots$ is the ratio of the frequencies of the first-order primary wave components for the resonant interaction. These components, however, are simultaneously undergoing self-interactions, the wave frequencies measured are a little higher than the frequencies of the primary waves. The *measured* frequency ratio at which resonance is observed is consequently a little different from the value $1{\cdot}7356\ldots$, as inspection of our results will show. The reconciliation is described by Longuet-Higgins & Smith in the accompanying paper, and there is no need to discuss it further here. Secondly, the response of the system to nearly resonant conditions is, as in all resonant systems, a function which becomes more sharply tuned as the interaction distance increases. Again, the elements of the theory are given in the paper by Longuet-Higgins & Smith; it will be noted that the observations to be described are consistent with this behaviour.

3. The experimental apparatus

It is essential in any experimental undertaking of this nature that conditions be precisely controlled. Accordingly, the wave tank and the associated generating and measuring devices were built specifically for this experiment. The wave tank itself was built of steel and glass, accurately levelled and squared. The interior dimensions are 11 ft. square by 4 ft. deep. It is supported on sixteen concrete columns above a firm concrete floor over solid earth. The structure is rather massive and stiff, to alleviate vibration and flexure problems.

Wave-makers and absorbing beaches are located along the four sides as shown in figure 2. The beaches are of plywood sheets, sloping at an angle of about 15°, covered with a 3 in. layer of rubberized horsehair to eliminate backwash effects. The amplitude reflexion is less than 10 % at all usable frequencies. This figure could have been improved by lengthening the beaches and making the slope more gradual, but this would have intruded greatly upon the already small working area.

The primary wave generators are of the plunger type. The smaller (σ_1) plunger is rectangular in cross-section; the larger trapezoidal with the front face sloping at 20° to the vertical. They are of ribbed plywood construction for lightness, covered with fibreglass for smoothness and water-proofing. The intersection of the two plungers is a sliding contact to prevent unwanted disturbances from propagating out into the working area as a result of end effects. Both plungers are driven vertically in a nearly sinusoidal motion by independent five h.p. synchronous motors through a variable spacing pulley and V-belt system and reduction worm gears. Frequencies of both plungers are individually and continuously adjustable over a range of $\frac{1}{2}$ to 4 strokes per second. The amplitudes of the strokes are individually and continuously adjustable from zero to 6 in., peak to peak. Stability of the generating frequency is within 0·1 % over a period of several hours; reproducibility of a given setting is within the same limits. Visual estimates indicate the wave crests produced by each plunger are uniform and straight, closely representing ideal two-dimensional (long crested) waves.

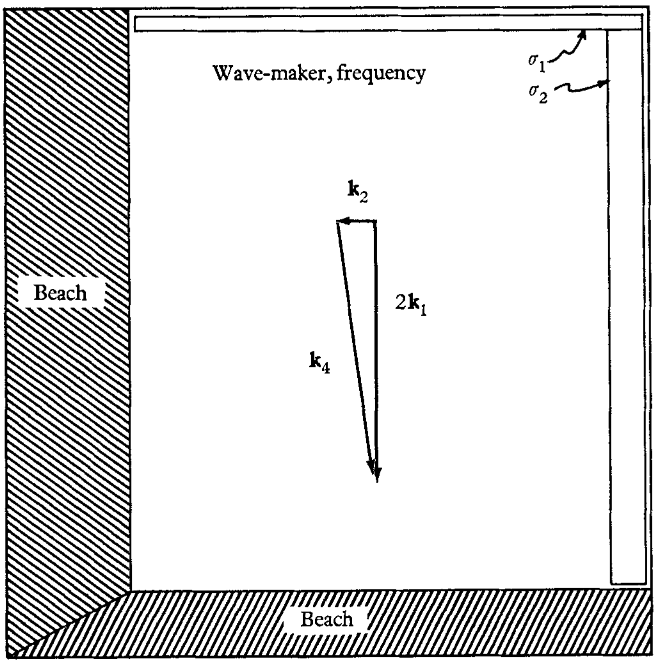

FIGURE 2. Diagram of the wave tank. The arrows identify the directions of the wave-numbers of interest.

Frequency measurements are made with a simple photocell circuit and an electronic counter. The frequencies of the waves, of course, are exactly those of the plungers. The entire plunger mechanism is supported by a rigid structural steel frame such that no part touches the wave tank. This is absolutely necessary in order to prevent mechanical vibrations from being transferred to the water where they would appear as unwanted noise in the measured wave signal.

Measurements of the free-surface elevation were made by a capacitance probe of a new type. Since prior calculation shows that the maximum amplitude of the resonant tertiary wave will be about 1 mm in the presence of 10 mm primary waves, extreme sensitivity, linearity and low noise are necessary in the detection system. Nothing suitable for this type of measurement is commercially available. The probe finally adopted is very simple, and can be made in about 15 min. It is produced by drawing a Pyrex tube to a diameter of less than 1 mm, filling the tube with clean mercury, and sealing one end in a flame. The other end is broken off at a length of about 6 in., a piece of wire (preferably iron) is inserted partially into the mercury and sealed in with a room-temperature vulcanizing silicone rubber sealing compound. The assembly is glued into a modified BNC connector (UG 88 C/U), the iron wire being soldered to the centre conductor pin. The resulting cylindrical capacitor has a capacitance of approximately 30 pF/cm in tap water.

This type of capacitance probe has many advantages over similar types used before (e.g. enamelled wire or teflon-coated wire). The high dielectric constant of glass increases the unit capacitance and so the sensitivity. The glass absorbs almost no moisture, so its normally very high leakage-resistance remains constant. This is crucial; variable characteristics require constant recalibration. The thickness of the glass wall is remarkably uniform, and there are no bumps or discontinuities such as those appearing in coated wire. An added and unexpected advantage is that if the probe and the water surface are kept sufficiently clean, there is no problem of meniscus reversal. When made in these short lengths for small scale laboratory studies, the probe is sufficiently rigid that it need be supported from only one end.

The probe is used as the capacitance element in a grounded capacitance blocking oscillator. Changes in capacitance (ideally directly proportional to the instantaneous surface elevation) modulate the repetition frequency of the output pulses. This modulated pulse train is detected by standard methods,† the output of the detector varying linearly with surface elevation. Calibration is accomplished dynamically by oscillating the probe in and out of still water with known amplitudes. The overall sensitivity of the system is about 0·7 V/mm wave amplitude at all frequencies of interest in the experiment. Linearity, as determined by static calibration with a micrometer traverse and digital voltmeter, is within 0·01 mm deviation from the best straight-line fit as a result of the uniformity of the probe and the linearity of the associated electronics. During the course of the measurements, the system was recalibrated at regular intervals. The sensitivity never changed by more than 2 %, and this is attributed to the ageing of the timing resistor in the blocking oscillator. Replacement restored the original figure. One probe was used almost daily for over a year, a tribute to the ruggedness of the device.

Actual measurement of wave heights is accomplished by passing the output signal from the wave detector through a sharply tuned band pass filter of the Wien bridge type (Dytronics, Model 720). The sharpness of the filter characteristic is adjusted to give 40 dB rejection of the frequency twice that and half that to which the filter is tuned. The centre frequency of the filter is set by comparison with an external low-frequency sine-wave oscillator adjusted precisely to the desired frequency with the aid of an electronic counter, and tuning the filter for 180° phase shift. The time average of the filtered signal is determined by squaring with a Philbrick Multiplier (Model MU/DV) and integrating over a large number of periods with an electronic integrator.

With this apparatus, an experiment can be performed much along the lines as described by Longuet-Higgins (1962). In the next section, the details of the procedure and the results will be presented.

† See, for instance, Huber (1958).

4. The initial linear growth

According to the simple theory, and as given by Longuet-Higgins & Smith (1966, equation (A 17)) and (2.12) above, the growth of the resonant tertiary wave is given by

$$a_4/d = (a_1k_1)^2\,(a_2k_2)\,G(r,\theta)\left|\frac{\sin\delta kd}{\delta kd}\right|, \tag{4.1}$$

where a_1 and a_2 are the amplitudes of the primary waves, assumed constant in the initial stages of growth. δk is half the difference between $k_4 = (4k_1^2+k_2^2)^{\frac{1}{2}}$ and the wave-number computed from $(2\sigma_1-\sigma_2)^2/g$. δk can also be written approximately as $\delta k = -0{\cdot}249\delta rk_4$, for small departures of r from r_0, for purposes of calculation. d is the distance over which the interaction takes place, and is measured in the direction of propagation of the k_4 wave. $G(r,\theta)$ is the interaction constant which depends on the frequency ratio $r = \sigma_1/\sigma_2$ and the angle of intersection θ of the primary waves. For 90° intersection, $r_0 = 1{\cdot}7356$, and $G(r_0, \frac{1}{2}\pi) = 0{\cdot}442$, as shown by Longuet-Higgins & Smith (1966). They further show that for variations of r over a range of 1·4 to 2·1, $G(r, \frac{1}{2}\pi)$ varies little from this value, so will be treated as a constant here, independent of r. Note that when $\delta k = 0$ $(r = r_0)$, the growth of the resonant wave is linear with d.

The experiment is divided into three separate series. For series I, the amplitude a_2 is constant, 8·95 mm, and the frequency $f_2\,(= \sigma_2/2\pi)$ is kept constant at 1·536 cycles/sec. The frequency ratio r is varied over a range of 1·5–2·2 by varying the speed of plunger number 1. Over this range of frequencies the maximum slope a_1k_1 remained approximately 0·1 For series II, the amplitude and frequency a_2 and f_2 are the same as in series I, but the stroke of plunger 1 is decreased just enough to decrease the maximum slope by a factor of $\sqrt{2}$ less than in series I. Measurements are still taken over the same range of frequency ratios, however. In series III, all the frequencies are increased by slightly greater than 10 %. f_2 is kept constant at 1·690 cycles/sec, and a_2 is reduced to 8·40 mm, and again the same frequency ratio is examined. The reason for this increase will be made clear later. For series I and II, detailed measurements are made at five points in the tank, for which d = 81·4, 107, 137, 168 and 198 cm. Beyond this, the beaches have an interfering effect.

The results of the measurements of series I are shown in figures 3–7 which show a dimensionless value of a_4 as a function of frequency ratio r. According to (4.1), with G assumed constant, the experimental points should closely approximate the shape of the curve $|\sin\delta kd/\delta kd|$, especially in the vicinity of r_0. Using the approximation of Longuet-Higgins & Smith, $\delta k = -0{\cdot}249\delta rk_4$, with k_4 chosen to be the value necessary to satisfy the resonance conditions $(k_4 = (4k_1^2+k_2^2)^{\frac{1}{2}})$, then for series I and series II the response function can be written approximately as

$$\left|\frac{\sin(0{\cdot}139\delta rd)}{(0{\cdot}139\delta rd)}\right|.$$

It is evident that as d increases, the centre lobe of the response function should become sharper, a characteristic width being inversely proportional to d, but the function should always have the same maximum value. The dashed curve in each of the figures 3–7 represents the calculated response function.

Figure 3 shows the results of the measurements at $d = 81{\cdot}4$ cm. In determining the ordinates, the values of a_1 and a_2 were measured for every point, as well as the amplitude a_4. Wave-numbers are calculated from the infinitesimal relation $k = \sigma^2/g$, and no attempt is made yet to correct for finite-amplitude effects. Each of the amplitude measurements has, however, been corrected for the inevitable electronic noise. Furthermore, when tuning the Wien bridge filter on any spectral line, the presence of neighbouring lines produces some contribution because of the shape of the filter characteristic. All amplitude measurements

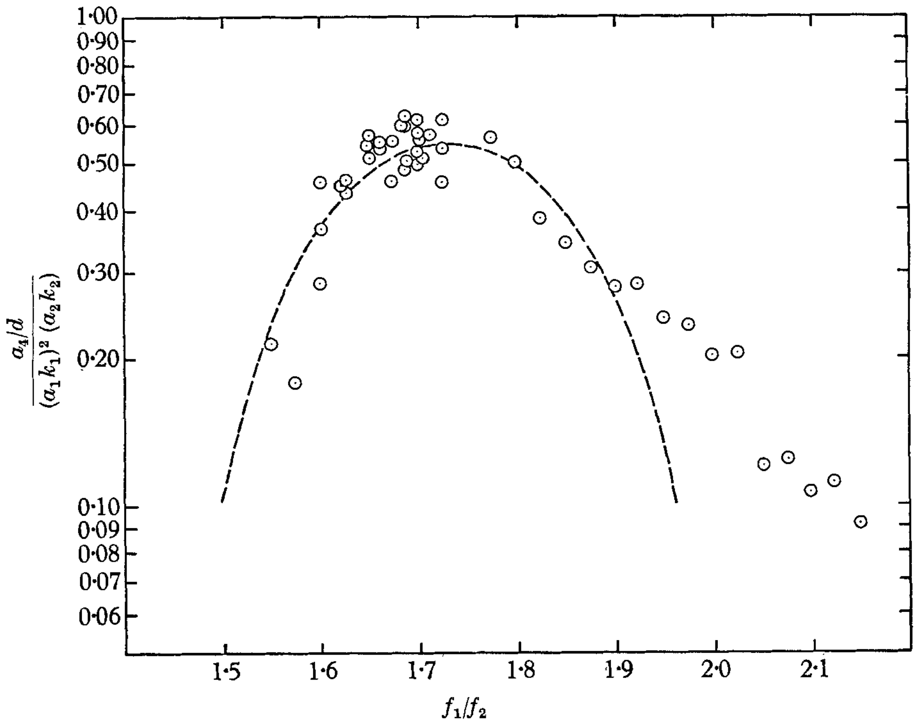

FIGURE 3. The resonant response at $d = 81{\cdot}4$ cm, series I.

have been corrected for this effect of the filter shape. Each of the points on this figure (and the succeeding four) is the average of at least 100 separate twenty-five second integrations. The large number of points is the result of several separate sweeps through the indicated frequency ratio range, separated in time by as much as one month to determine whether or not the results could be repeated.

Experimental values for the constant $G(r, \frac{1}{2}\pi)$ and the resonant frequency ratio r_m are determined by obtaining the best fit of the calculated response function to the experimental points (by eye). The location of this best fit is shown by the dashed line. The resonant frequency ratio r_m, that at which the maximum occurs, for figure 3 is $1{\cdot}73$, and the peak (which should correspond to the theoretical value of G, namely $0{\cdot}442$) is $G_m = 0{\cdot}55$.

Figure 4 shows the results of measurements at $d = 107$ cm. The response function has become sharper, as has the grouping of the experimental points. For this station, $G_m = 0{\cdot}57$ and $r_m = 1{\cdot}74$.

Figure 5 shows the results at $d = 137$ cm. The response function, calculated and experimental, is sharper still. Here, $G_m = 0{\cdot}55$ and $r_m = 1{\cdot}745$. For $d = 168$ cm, figure 6 shows further sharpening, and $G_m = 0{\cdot}55$, $r_m = 1{\cdot}75$. For $d = 198$ cm, the response is sharper again. For this last station, $G_m = 0{\cdot}57$ and

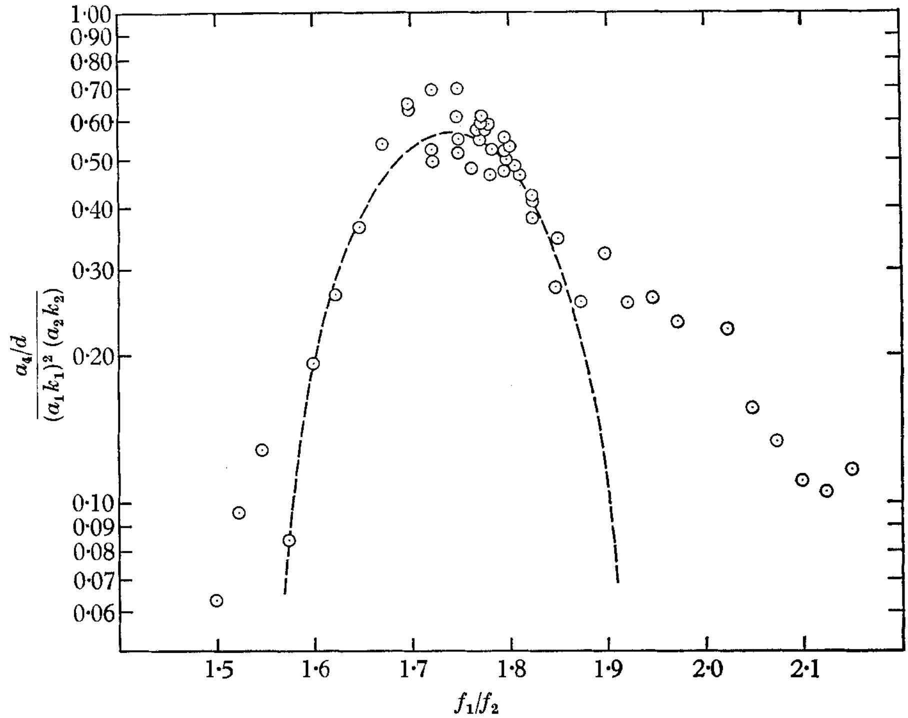

FIGURE 4. The resonant response at $d = 107$ cm, series I.

$r_m = 1{\cdot}78$. Table 1 summarizes the results of series I in detail. Here, a_4 and a_4k_4 are determined from the measured values of G_m. k_1 and k_4 correspond to the values of the wave-numbers at the experimentally-determined resonant frequency ratio.

According to (4.1) the growth rate of the resonant wave is proportional to the square of the maximum slope of the primary wave. If, everything else being held constant, the amplitude a_1 is decreased by a factor of $\sqrt{2}$, the resulting growth rate of the resonant a_4 wave should be halved. Series II was an investigation of this prediction. Measurements were made at the same five stations over approximately the same range of frequency ratios, and repeatability determined in the same manner as in series I. The results, when plotted as in figures 3–7, are virtually indistinguishable from the results of series I in all details, and need not be shown here. The locations and heights of the peaks of the response functions are identical, and the experimental scatter is within the same limits. This indicates that the growth rate is indeed halved. Figure 8 shows the growth of the resonant

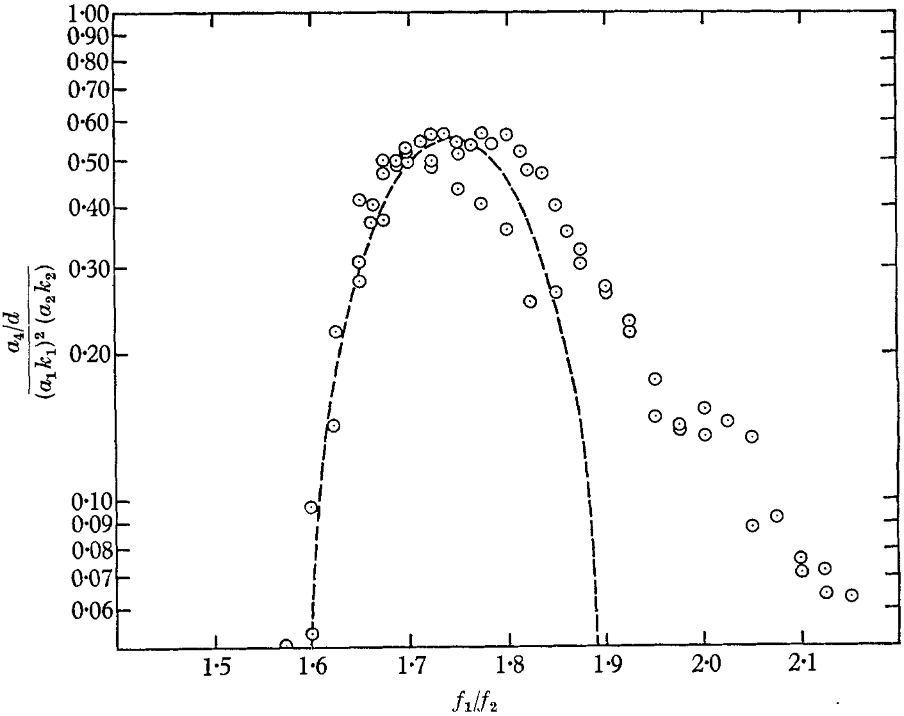

FIGURE 5. The resonant response at d = 137 cm, series I.

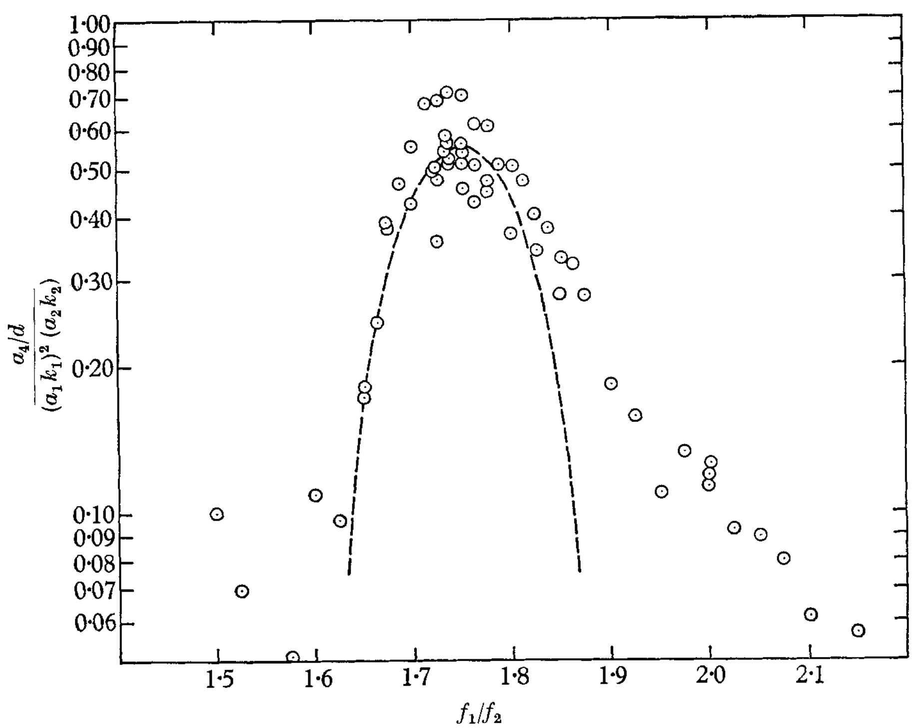

FIGURE 6. The resonant response at d = 168 cm, series I.

wave with distance for both series I and series II. The actual best fit to the growth rate in series II is 0·516 times that in series I, well within any experimental error of the expected value 0·5.

To guard against the possibility that the results of series I and II are influenced by reflexions or strange harmonic structure in the finite-size tank, the measurements of series III have been performed at frequencies and wave-numbers not commensurate with the previous series. Approximately the same range of frequency *ratios* is examined, however, and a comparison of the results measured at d = 198 cm is shown in figure 9. The ordinate and abscissa have been made

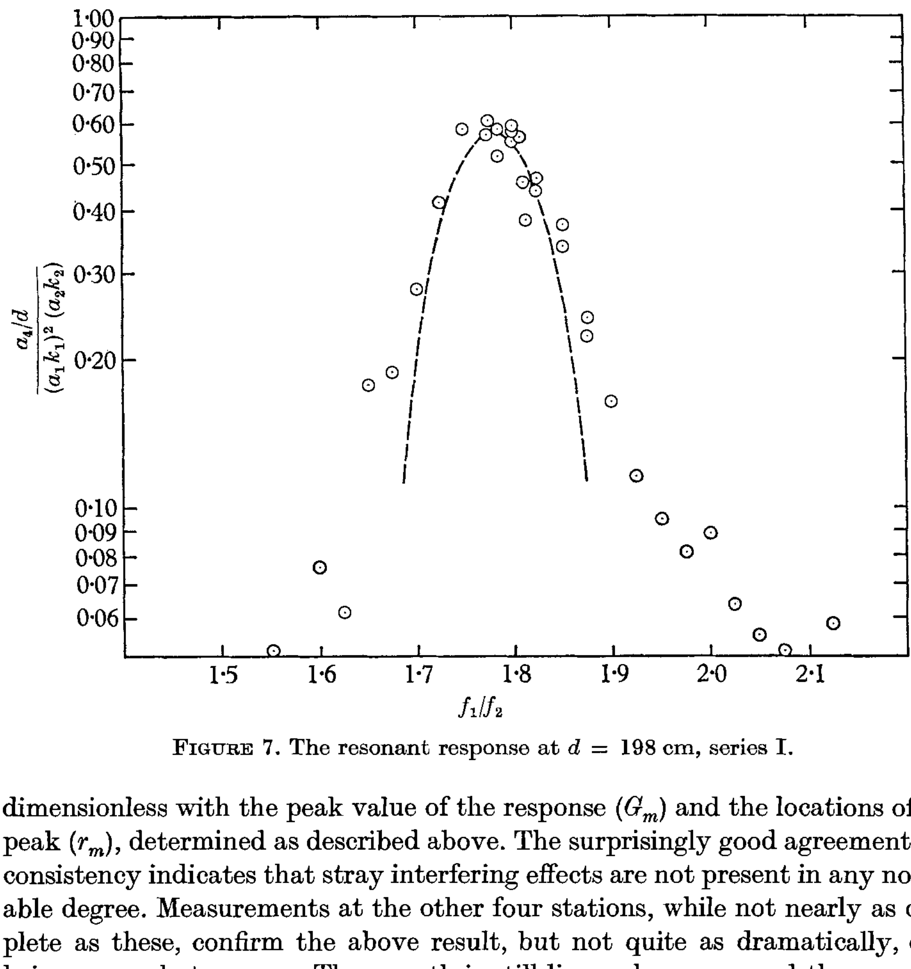

FIGURE 7. The resonant response at d = 198 cm, series I.

dimensionless with the peak value of the response (G_m) and the locations of the peak (r_m), determined as described above. The surprisingly good agreement and consistency indicates that stray interfering effects are not present in any noticeable degree. Measurements at the other four stations, while not nearly as complete as these, confirm the above result, but not quite as dramatically, data being somewhat sparser. The growth is still linear, however, and the measurements exhibit a similar characteristic shape.

So far, attention has been confined to measurements of the resonant wave at frequency $2\sigma_1 - \sigma_2$ and the primary waves at frequencies σ_1 and σ_2. Other harmonics are however present in the tank. By the nature of the basic non-linearity of gravity waves, presence of bounded second-order harmonics ($2\sigma_1$, $2\sigma_2$, $\sigma_1 \pm \sigma_2$) and third-order harmonics ($3\sigma_1$, $3\sigma_2$, $2\sigma_1 + \sigma_2$, $\sigma_1 \pm 2\sigma_2$) is assured, as well as harmonics of higher order which are of no interest here. A separate set of measure-

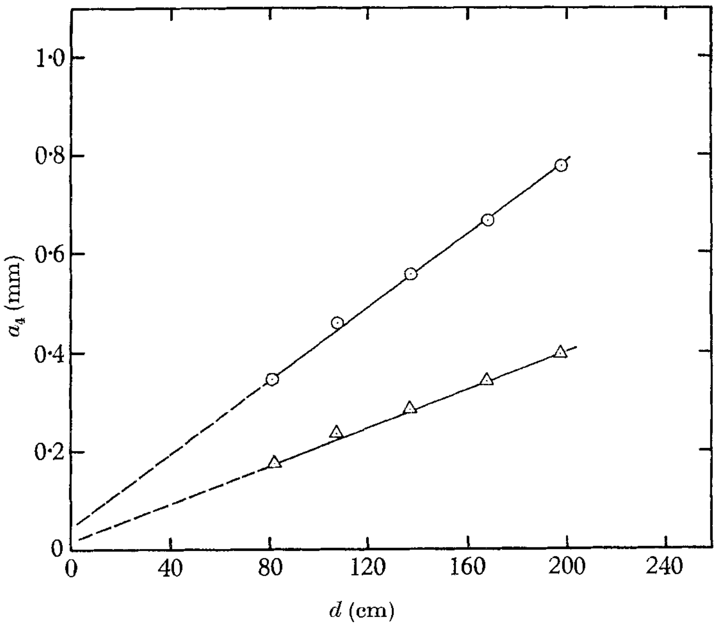

FIGURE 8. The measured growth of a_4. ⊙, Series I; △, series II.

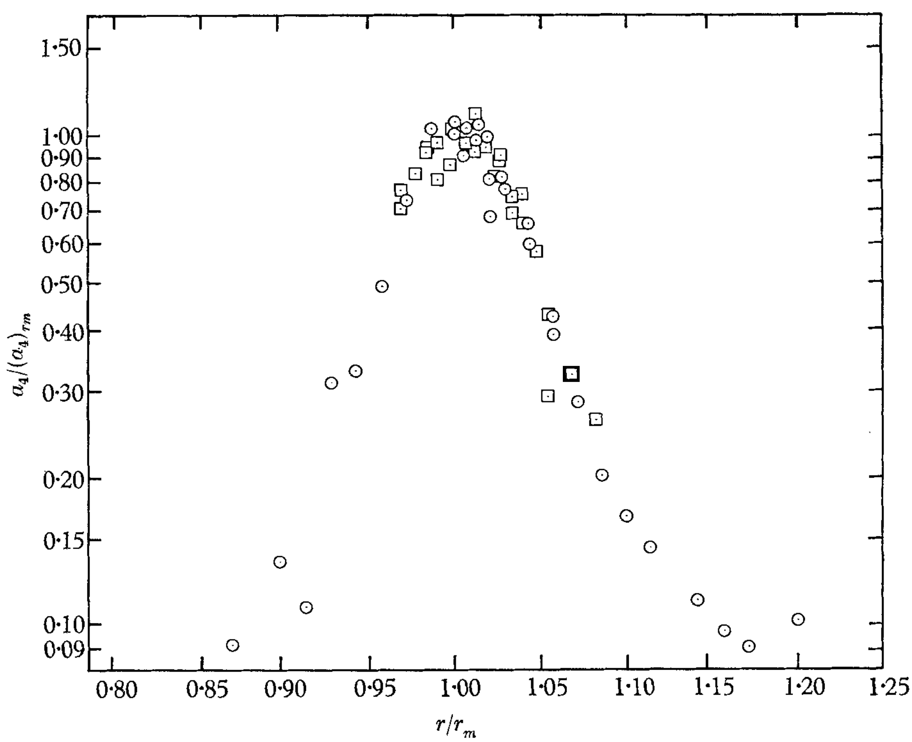

FIGURE 9. Comparison between resonant responses for series I and III. For series III, r_m = 1·775. ⊙, Series I; ⊡, series III; d = 198 cm.

ments has been undertaken to determine the harmonic structure for several sets of primary frequencies corresponding to the three series described above.

Figure 10 is a comparison of the amplitude spectra between series I (upper figure) and series II (lower figure), both measured at $d = 137$ cm. In both cases, the frequency of wave-maker 1 is set so that the frequency ratio corresponds to the theoretically predicted critical frequency ratio $r_0 = 1{\cdot}7356$. This is quite close

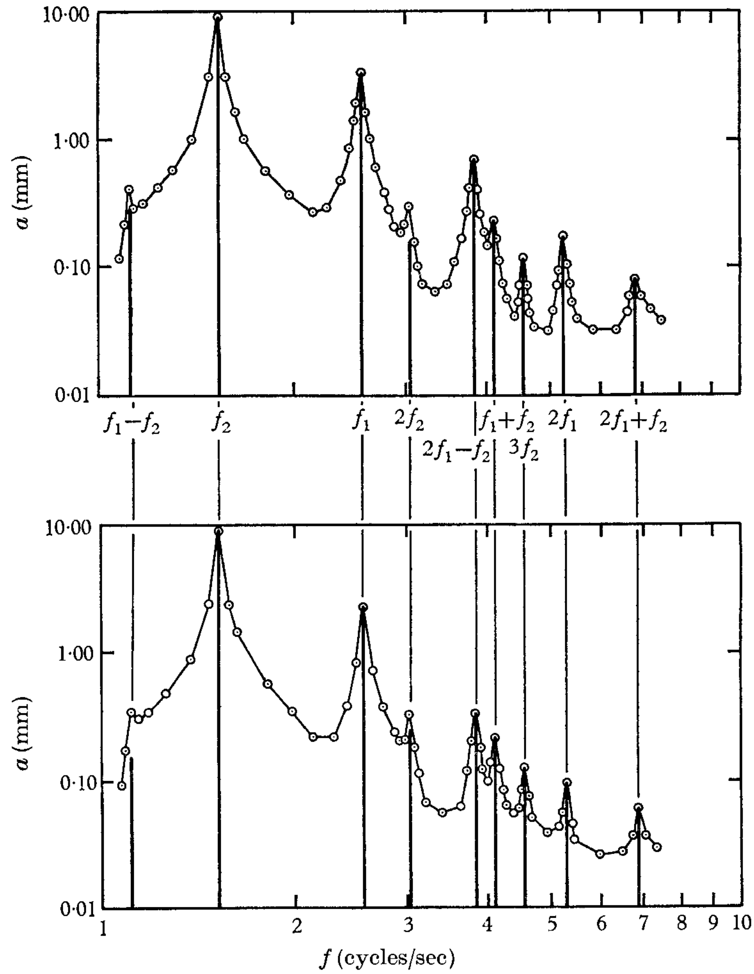

FIGURE 10. Amplitude spectra measured at $d = 137$ cm for series I (upper) and series II (lower), both on resonance.

to the measured resonant frequency ratio (see table 1), for both series, and the measurements are taken to be representative of the spectral content at resonance. All the harmonics that are measurable in the frequency range from 1·0 to 8 cycles/sec are identified in the margin between the two figures. The circles represent actual data points as measured with the use of the Wien bridge filter. The heavy vertical lines represent the actual spectral content, assuming, of course, that the spectra are composed of discrete harmonics superimposed on background

d (cm)	k_1 (cm^{-1})	k_2 (cm)$^{-1}$	k_4 (cm)$^{-1}$	a_1k_1	a_2k_2	a_4k_4	a_1 (cm)	a_2 (cm)	a_4 (cm)	r_m	$G_m(r_m, \frac{1}{2}\pi)$
81·4	0·284	0·0949	0·578	0·0945	0·0850	0·0198	0·334	0·895	0·035	1·73	0·55
107	0·287	0·0949	0·585	0·0934	0·0850	0·0268	0·328	0·895	0·046	1·74	0·57
137	0·289	0·0949	0·587	0·093	0·0850	0·0325	0·322	0·895	0·055	1·745	0·55
168	0·290	0·0949	0·590	0·092	0·0850	0·0392	0·317	0·895	0·066	1·75	0·55
198	0·300	0·0949	0·610	0·090	0·0850	0·0474	0·300	0·895	0·078	1·78	0·57

$$k_4 = k_2(4r_m^4+1)^{\frac{1}{2}}, \quad k_1 = k_2 r_m^2, \quad a_4 = (a_1k_1)^2\,(a_2k_2)\,dG_m(r_m, \tfrac{1}{2}\pi).$$

TABLE 1. Summary of results of series I. $G_m(r_m, \frac{1}{2}\pi)$ and r_m are the experimentally-determined values of the interaction constant and resonant frequency ratio.

(electronic) noise. If the filter characteristic (transfer function) is applied to the complete discrete spectra shown, the resulting responses very nearly duplicated the measured points, agreement being particularly good in the vicinity of spectral peaks.† Of particular importance in comparing these two spectra are the relative sizes of a_1 (at f_1) and a_4 (at $2f_1 - f_2$). According to (4.1) and as previously

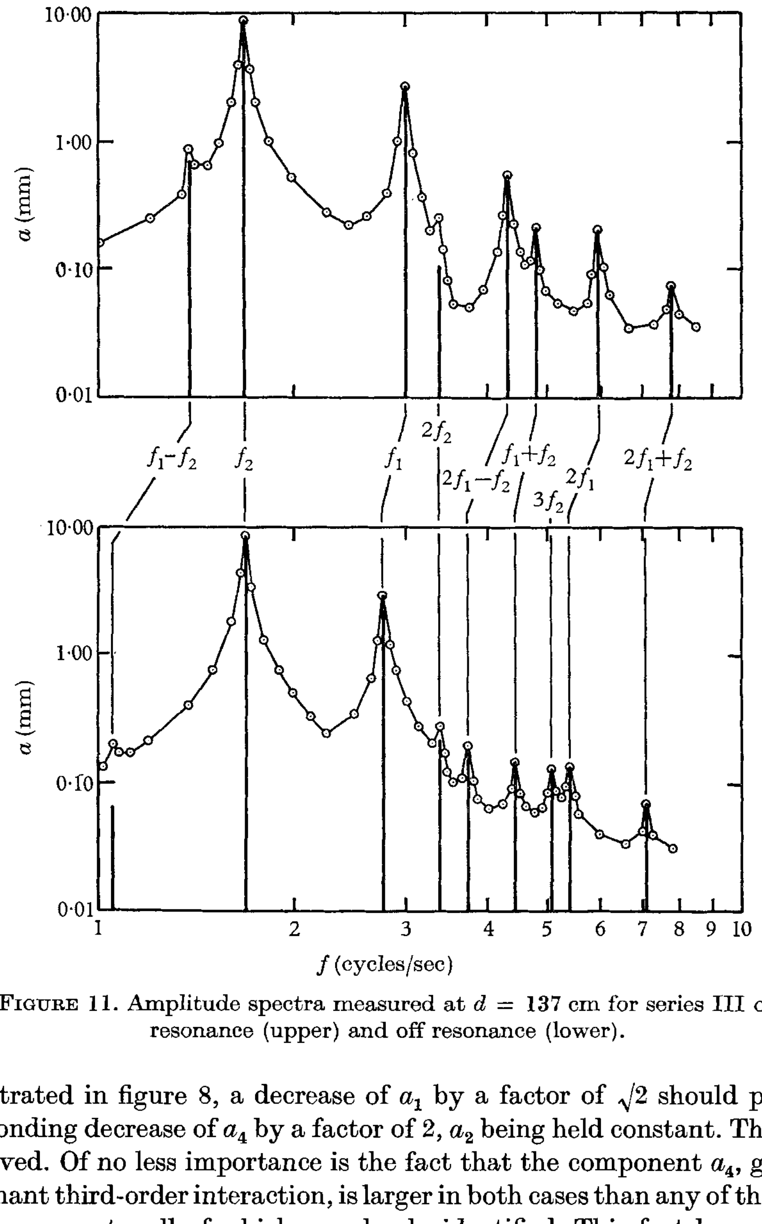

FIGURE 11. Amplitude spectra measured at $d = 137$ cm for series III on resonance (upper) and off resonance (lower).

demonstrated in figure 8, a decrease of a_1 by a factor of $\sqrt{2}$ should produce a corresponding decrease of a_4 by a factor of 2, a_2 being held constant. This indeed is observed. Of no less importance is the fact that the component a_4, generated by resonant third-order interaction, is larger in both cases than any of the second-order components, all of which are clearly identified. This fact becomes more evident at larger values of d, since a_4 is increasing. It is notable that *none of the*

† In fact, the distribution of points about the highest spectral peak (at f_2) represents very closely the filter shape.

second-order components, nor the primaries, engaged in any measurable growth (or decay) across the tank. This is based on more detailed information collected during the course of series I. The other third-order components are too small to be measured consistently.

Figure 11 is a comparison of two spectra for series III. The upper spectrum is on resonance, and the lower, off resonance. The detuning is accomplished by decreasing f_1, while keeping the amplitudes of the primaries the same. The important point here is the observation that the resonant component $(2f_1 - f_2)$ is greatly diminished in the off-resonance case.

5. Some comments

It should be emphasized that the results of the preceding section represent what is actually present in the wave tank for any particular frequency settings. The only corrections that have been applied are those concerning the more obvious electronic influences, and have been discussed above. It is the purpose of this brief section to comment on the relation between the observations and the theory.

The most apparent difference is in the growth rate, as can be seen by comparing the measured values of the interaction constant $G_m(r_m, \frac{1}{2}\pi)$ with the theoretical value first calculated by Longuet-Higgins (1962). The theoretical and measured growth rates differ by about 20%. This is about the upper limit of possible systematic errors in measurement of absolute amplitudes, and no strenuous attempt will be made here to reconcile the two figures. Most important in this regard, however, is the surprisingly good consistency among the observations from point to point within the tank. That the distribution of relative levels, as presented in figures 3–7 and figure 9, is in such good agreement with the theoretically determined response functions can be taken as evidence that the resonance mechanism is of fundamental importance in the dynamics of energy transfer. This and the linear growth demonstrated in figure 8 definitely rule out the possibility of a steady state under resonant conditions.

The other significant difference is in the observed values of the critical frequency ratio r_m. From table 1 it is evident that frequency ratio for maximum resonant response is increasing with the distance of propagation, but is remarkably close to the theoretical r_0. Longuet-Higgins & Smith (1966) also noticed this effect, but their departures from r_0 are much larger than ours. They rightfully attribute this discrepancy to other finite amplitude (but non-resonant) effects, such as self interaction (the Stokes correction), mutual interaction, and the influence of surface tension and finite depth. The first two effects arise directly from the terms under the summation signs in the right-hand side of (2.4), as explained previously, which arise at third order. The other two effects influence the wave-number–frequency relationship directly, and are present at all orders of approximation. Longuet-Higgins & Smith present a detailed analysis of the corrections to be applied to reconcile this difficulty, with some success. The same system of corrections can be applied to the present results, with the exception of that for finite depth, which turns out to be insignificant for our case. The tendency of corrections of these types applied to series I, II and III is to make the discrepancy smaller, but the maximum influence is not greater than about 2%, which hardly justifies the effort involved, and is certainly smaller than the graphical errors involved in determining r_m in the first place. The reason that our critical frequency ratios are so close to the predicted value is that the slopes of the primary waves have been made as small as can be tolerated within the present resolution of the detection system.

In light of the success of these experiments, it seems prudent to clear up a possible confusion generated by the designation of the growing wave as a 'resonant tertiary wave'. The distinction between the terms 'third order' and 'tertiary', as used in the present context, should be made. If strict concepts of order are followed, then this wave is no longer of third order by the time it has progressed half way across the tank. Indeed, in the limited facility here, this observed growth shows no signs of stopping, so an upper limit to its size cannot as yet be determined experimentally, even though energy considerations place an absolute upper limit on its amplitude. The mechanism here is the same as that discussed by McGoldrick (1965) in which it is shown by numerical example that two capillary-gravity waves can create a resonant wave whose maximum slope becomes greater than either of the initial slopes in a very short time, whereupon the process reverses itself in a periodic manner in such a way as to keep the total energy per unit projected surface-area constant. Similarly in the present case, the interaction is to be interpreted as being among three waves of arbitrary (but inter-related) amplitudes. The extended analysis of § 2 above is based on precisely this interpretation, the aim of the analysis being the prediction of the finite amplitudes of the three (or four, as the case may be) interacting modes as a function of time under a constant energy constraint. So the adjective 'third order' should not be used to describe the interacting waves themselves. It is justifiable, however, to describe the entire mechanism as a *tertiary resonant interaction*, for the simple reason that the dynamical terms in the governing equations that are responsible for this time-dependent energy transfer are of third order in the mathematical hierarchy.

This work was supported by the Fluid Dynamics Branch of the Office of Naval Research under contracts Nonr 248(56) and Nonr 4010(02). In addition, the first author received partial support during the early stages of this investigation from the National Science Foundation Fellowship Programs. We are particularly indebted to Dr M. S. Longuet-Higgins for supplying us with a preliminary copy of his experimental results.

REFERENCES

Ball, F. K. 1964 Energy transfer between external and internal gravity waves. *J. Fluid Mech.* **19**, 465–78.

Benney, D. J. 1962 Non-linear gravity wave interactions. *J. Fluid Mech.* **14**, 577–84.

Bretherton, F. P. 1964 Resonant interaction between waves, the case of discrete oscillations. *J. Fluid Mech.* **20**, 457–79.

Hasselman, K. 1962 On the non-linear energy transfer in a gravity wave spectrum. Part 1. General theory *J. Fluid Mech.* **12**, 481–500.

HASSELMAN, K. 1963*a* On the non-linear energy transfer in a gravity wave spectrum. Part 2. Conservation theorems; wave-particle analogy; irreversibility. *J. Fluid Mech.* **15**, 273–81.

HASSELMAN, K. 1963*b* On the non-linear energy transfer in a gravity wave spectrum. Part 3. Evaluation of the energy flux and sea-swell interaction for a Newmann spectrum. *J. Fluid Mech.* **15**, 385–98.

HUBER, E. A. 1958 Improved system for the measurement of heights of water waves. *Report* no. I-78 Control Systems Laboratory. University of Illinois, Urbana, Illinois.

LONGUET-HIGGINS, M. S. 1962 Resonant interactions between two trains of gravity waves. *J. Fluid Mech.* **12**, 321–32.

LONGUET-HIGGINS, M. S. & PHILLIPS, O. M. 1962 Phase velocity effects in tertiary wave interactions. *J. Fluid Mech.* **12**, 333–36.

LONGUET-HIGGINS, M. S. & SMITH, N. D. 1966 An experiment on third-order resonant wave interactions. *J. Fluid Mech.* **25**, 417.

MCGOLDRICK, L. F. 1965 Resonant interactions among capillary-gravity waves. *J. Fluid Mech.* **21**, 305–31.

PHILLIPS, O. M. 1960 On the dynamics of unsteady gravity waves of finite amplitude. Part 1, The elementary interactions. *J. Fluid Mech.* **9**, 193–217.

PIERSON, W. J. 1961 Comments on a paper by O. M. Phillips, appearing in *Proceedings of a Conference on Ocean Wave Spectra, Easton, Md.*, 1961. Published as *Ocean Wave Spectra*, pp. 180–6 and 187–8. Prentice-Hall, Inc., Englewood Cliffs, N.J. (1963).

THORPE, S. A. 1966 On wave interactions in a stratified fluid. *J. Fluid Mech.* **24**, 737.